

REVIEW ARTICLE | MARCH 01 2024

Multiscale modeling and simulation of turbulent flows in porous media

Yan Jin   ; Andrey V. Kuznetsov 



International Journal of Fluid Engineering 1, 010601 (2024)

<https://doi.org/10.1063/5.0190279>



Featured

Multiscale modeling and simulation of turbulent flows in porous media

Cite as: *Int. J. Fluid Eng.* **1**, 010601 (2024); doi: [10.1063/5.0190279](https://doi.org/10.1063/5.0190279)

Submitted: 5 December 2023 • Accepted: 4 February 2024 •

Published Online: 1 March 2024



View Online



Export Citation



CrossMark

Yan Jin^{1,a)}  and Andrey V. Kuznetsov² 

AFFILIATIONS

¹Institute of Multiphase Flows, Hamburg University of Technology, Hamburg 21073, Germany²Department of Mechanical and Aerospace Engineering, North Carolina State University, Raleigh, North Carolina 27695-7910, USA^{a)}Author to whom correspondence should be addressed: yan.jin@tuhh.de

ABSTRACT

Numerical simulation is an important tool for understanding the physics of flows in porous media and for making predictions. The state of the art of multiscale modeling and simulation of turbulent flows in porous media is reviewed in this paper. Numerical simulations of flows in porous media can be classified as microscopic simulations, in which both macroscopic and pore-scale flows are directly resolved, and macroscopic simulations, in which the pore-scale motions are modeled while the volume-averaged equations are solved. Studies in the past few years have shown that microscopic simulations improve the understanding of turbulent flows in porous media considerably; this motivates the development of more efficient and more accurate turbulence models for macroscopic simulations. On the basis of this review, we believe that simulation of flows with higher Reynolds numbers, understanding the transport of macroscopic turbulence, modeling of turbulent flows in inhomogeneous and anisotropic porous media, simulation of compressible and multiphase turbulent flows in porous media, and fluid–structure interaction in deformable porous matrices are important topics to be studied in the future.

© 2024 Author(s). All article content, except where otherwise noted, is licensed under a Creative Commons Attribution (CC BY) license (<http://creativecommons.org/licenses/by/4.0/>). <https://doi.org/10.1063/5.0190279>

I. INTRODUCTION

A porous medium is a material that contains pores (voids). The skeletal part of the porous medium is often solid and is therefore called the solid matrix or porous matrix. The pores are often filled with fluids (gases or liquids). The transport of fluids in porous media is an important process in many applications, including CO₂ sequestration in deep saline aquifers (Benson and Cole, 2008; Huppert and Neufeld, 2014), energy extraction from geothermal reservoirs or the ambient ground (Ghoreishi-Madiseh *et al.*, 2013), enhanced oil/gas recovery (Gbadamosi *et al.*, 2019), transport of groundwater contaminants (Patil and Chore, 2014), and stability of snow against avalanches (Nield and Simmons, 2019).

Convection in porous media is usually laminar, since it often has a low pore-scale Reynolds number (Re_d) defined by the pore size d and the mean flow velocity u_m . However, when Re_d is of the order of 100 or higher, the flow within the pores becomes turbulent. An example of an application to which this is relevant is thermal energy storage systems that use rocks/bricks for storing thermal energy (Odenthal *et al.*, 2014). The processes of heat charging and

discharging in such energy storage systems are often driven by mixed (combined forced and natural) convection. Rocks or bricks have low thermal conductivity, resulting in very slow processes of charging and discharging. To overcome this disadvantage, the size of the porous element and the velocity of the fluid may be adjusted to make the flow fully turbulent. If the porous medium can be approximated by a bank of tubes, then the relationship between the Nusselt number and the Reynolds number changes from $Nu \sim Re_d^{0.36}$ for $Re_d < 300$ to $Nu \sim Re_d^{0.64}$ for a fully turbulent flow ($Re_d > 300$); see *Engineering Sciences Data Unit* (1984). The heat transfer is efficiently enhanced by the turbulence.

Turbulence in porous media might also occur in packed bed reactors in chemical engineering problems (Shams *et al.*, 2014; Dave *et al.*, 2018; and Lucci *et al.*, 2017). For example, the pore-scale Reynolds number for a nuclear pebble bed reactor can reach the order of 10^5 (Dave *et al.*, 2018), which is considerably higher than the Reynolds number for laminar–turbulent transition. Likewise, flows in a catalyst packed bed can also reach the order of 10^4 (Lucci *et al.*, 2017).

Another important application of turbulence in porous media is in canopy flows. The porous canopies can be made of trees, vegetation, buildings, or wind farms (Meroney, 2007). Canopies usually have large porosity values ϕ [typically $\phi > 90\%$; see Ghisalberti and Nepf (2009)] and extremely high Reynolds numbers. For example, Belcher (2005) studied canopy flows in urban areas, which have pore-scale Reynolds number $Re_d = 5000$. Turbulence in plant canopies can have Reynolds numbers up to 10^5 in the upper part of well-ventilated canopies and as low as 10^2 near the ground (Belcher *et al.*, 2012).

Besides the classical turbulent flows introduced above, flow instabilities might also occur in natural convection in porous media at high Rayleigh numbers. Natural convection flows in porous media at large Rayleigh numbers are transient, chaotic, and random; these characteristics are similar to those of classical turbulence. However, transient natural convection in porous media can occur at very low pore-scale Reynolds numbers. These transient flows are called “pseudo-turbulence,” which is a term used to distinguish them from classical turbulence. “Pseudo-turbulence” of natural convection in porous media has important applications in CO₂ sequestration (Huppert and Neufeld, 2014), geothermal energy (Ghoreishi-Madiseh *et al.*, 2013), and enhanced oil/gas recovery (Gbadamosi *et al.*, 2019).

Driven by the need to solve industrial problems and understand physical problems in nature, there have been extensive studies of turbulent flows in porous media in the past few years. Computational fluid dynamics (CFD) is an important tool for understanding this process. According to the difference in the time and length scales of motions to be solved, CFD simulations of convection in porous media can be classified into microscopic and macroscopic simulations. In microscopic simulations, the motions smaller than the representative elementary volume (REV) should be calculated; thus, the detailed geometry of the porous elements must be considered. A pore-scale-resolved direct numerical simulation with a perfectly stirred reactor model (PSR-DNS) is a typical microscopic simulation. In a PSR-DNS, the microscopic governing equations (usually the Navier–Stokes equations) are solved directly without the introduction of additional models. A PSR-DNS method usually has higher accuracy than other simulation methods. However, only recently has it become possible to study turbulent flows in porous media with PSR-DNS methods owing to their extremely high computational cost (Chandesris *et al.*, 2013; Jin *et al.*, 2015; Uth *et al.*, 2016; Chu *et al.*, 2019; Rao and Jin, 2022; Wang *et al.*, 2021; 2022; and Srikanth *et al.*, 2021). Pore-scale-resolved large eddy simulation (PSR-LES) is another common microscopic simulation method. It has important applications owing to its moderate computational cost (Hutter *et al.*, 2011; Shams *et al.*, 2014; and Huang *et al.*, 2022).

Compared with microscopic simulations, macroscopic simulations of porous medium convection are more efficient. The macroscopic equations can be obtained by time and volume averaging (or sometimes only volume averaging) of the microscopic governing equations. Macroscopic simulation is the most widely used method for calculating turbulent flows in porous media in engineering applications owing to its low computational cost (Lee and Howell, 1991; Prescott and Incropera, 1995; Lage *et al.*, 1997; Kazerooni and Hanani, 2009; Kundu *et al.*, 2014; and de Lemos and Braga, 2003). The problem with macroscopic simulations is that strong assumptions

are often used to close the averaged momentum equation, leading to inaccuracy and uncertainty of the numerical solutions.

Despite the efforts made in recent years, microscopic simulation and macroscopic modeling of turbulent flows in porous media remain challenging tasks owing to the high complexity of the problem as well as the difficulty in validation. The purpose of this paper is to review the important work on multiscale modeling and simulation of turbulent flows carried out in the past few years. In the review, we consolidate and systemically analyze the knowledge on this topic that has been accumulated in the past years. We also discuss important unsolved problems that will need to be addressed in future work.

The structure of the paper is as follows. Following this introduction, microscopic simulation of turbulent flows in porous media is discussed in Sec. II. Then, the governing equations for macroscopic simulations are introduced in Sec. III. Section IV focuses on modeling of the macroscopic equations. Two types of turbulence models, macroscopic and microscopic turbulence models, are discussed in this section. Finally, a summary of the established knowledge and future issues is given in Sec. V.

II. MICROSCOPIC SIMULATION OF TURBULENT FLOWS IN POROUS MEDIA

Microscopic simulation of flows in porous media concerns simulations in which the pore-scale flows are directly resolved. DNS is the most accurate method for microscopic simulation. It is defined as a CFD simulation in which the Navier–Stokes equations are solved directly without the introduction of a turbulence model. DNS of turbulent flows in porous media requires the detailed pore-scale geometry to be resolved; thus, this DNS is also called pore-scale-resolved DNS (PSR-DNS).

In DNS, the following governing equations for incompressible flows are typically solved:

$$\frac{\partial u_i}{\partial x_i} = 0, \quad (1)$$

$$\frac{\partial u_i}{\partial t} + \frac{\partial(u_i u_j)}{\partial x_j} = -\frac{\partial p}{\partial x_i} + \nu \frac{\partial^2 u_i}{\partial x_j^2} + g_i, \quad (2)$$

where ν is the kinematic viscosity of the fluid. A constant applied pressure gradient g_i is often required to force the fluid to move. p is the kinematic pressure, defined as the ratio of the static pressure P to the constant density ρ . Compressibility of the fluid is rarely taken into account in flows in porous media. Instead, the Boussinesq approximation is usually used if the buoyancy force due to the density variation in natural convection needs to be considered. This frequent neglect of compressibility is partly because the Mach number Ma of flows in porous media is generally small ($Ma < 0.3$). However, it should be noted that fluid compressibility may have non-negligible effects when there are strong temperature or pressure variations.

A subgrid-scale (SGS) modeling term is sometimes added to the momentum equation to model small eddies to reduce the computational cost. The simulation then becomes a large eddy simulation (LES). LES also belongs to the class of microscopic simulations when the motions below the pore scale are resolved. Theoretically, the

pore-scale motions can also be solved by using Reynolds-averaged Navier–Stokes (RANS) simulations (Soulaine *et al.*, 2017; Ferdos and Dargahi, 2016; and Dave *et al.*, 2018). Jin and Herwig (2015) simulated flows in channels with rough walls (where the walls were covered with porous elements) using eight RANS models and compared the results obtained with those from DNS. The comparison revealed that the errors in the calculated friction coefficients exceeded 20% in all-the RANS results. It was demonstrated that even k - ϵ and Reynolds stress models could predict incorrect trends. Therefore, it is expected that PSR-RANS results may exhibit considerable uncertainties due to model errors when used to simulate turbulent flows in porous media. PSR-DNS and PSR-LES are more suitable for understanding the physics of turbulent flows in porous media.

We focus on continuum fluids (with Knudsen number $Kn < 0.01$) in this review. Therefore, standard boundary conditions can be applied in the PSR-DNS and PSR-LES. No-slip boundary conditions are imposed at the surfaces of solid obstacles. Most DNS and LES studies avoid using inlet boundary conditions, primarily because it is challenging to prescribe turbulent fluctuations at the boundaries. Periodic or no-slip boundary conditions are often utilized at the boundaries of porous media. With these boundary conditions, it is possible to obtain fully developed (statistically steady) flows for statistical analysis.

To resolve the intricate pore-scale geometry, PSR-DNS and PSR-LES are often conducted using a finite volume method (FVM), as demonstrated by Jin *et al.* (2015), Gasow *et al.* (2020), and Wang *et al.* (2021, 2022), or a lattice Boltzmann method (LBM), as shown by Liu *et al.* (2021; 2023), Li *et al.* (2022), and Diao *et al.* (2023). Finite difference methods and spectral-type methods are seldom used, owing to difficulties in resolving pore-scale geometry. Among these methods, the LBM, which has emerged in recent years, has demonstrated particular potential in PSR-DNS and PSR-LES of flows in porous media owing to its excellent parallelizability. However, further efforts are needed to enhance this method for broader applications, such as calculating compressible flows and using body-fitted meshes.

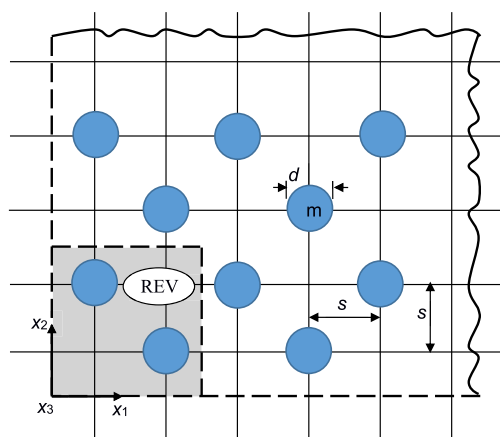


FIG. 1. Porous matrix (GPM) with representative elementary volumes REV for microscopic simulations.

Many microscopic simulation studies investigate flows in porous media with homogeneously distributed porous elements. In periodic problems, the computational domain is composed of representative elementary volumes (REV). REV are appropriately sized to accurately reflect the pore-scale properties of the entire volume in question (i.e., the porosity and permeability do not change if the volume is further enlarged). REV in fundamental studies are often constructed from simple geometries; for example, REV can be made of staggered arrangement of cylinders (Fig. 1) or spheres.

PSR-DNS and PSR-LES require the resolution of motions within both the pores and macroscopic elements, making them computationally intensive. For instance, Jin *et al.* (2015) employed 10^7 – 6×10^7 mesh cells to resolve each REV consisting of aligned bars, totaling 5×10^7 – 3.8×10^8 mesh cells for simulating turbulent flows in a matrix comprising six REV. Similarly, Uth *et al.* (2016) used 4800 mesh cells to resolve each REV composed of three-dimensional spheres. Wang *et al.* (2021; 2022) utilized 8.8×10^7 – 5.8×10^8 mesh cells to simulate turbulent flows partially obstructed by a porous medium. In a DNS study of pseudo-turbulence, Gasow *et al.* (2020; 2021; and 2022) employed 3600 mesh cells to resolve a two-dimensional REV, totaling up to 7.2×10^8 mesh cells.

The ratio of the pore scale and the macroscopic scale can be characterized by the Darcy number Da , defined as

$$Da = \frac{K}{H^2}, \quad (3)$$

where K is the permeability and H the length scale of the macroscopic geometry. Da for naturally occurring porous media can be very small. For example, Da for a CO₂ sequestration site can be of order 10^{-13} or even lower. By contrast, relatively large Da values are often used in PSR-DNS and PSR-LES to reduce computational cost. Da in the DNS study by Jin *et al.* (2015) is of order 0.1. The smallest Da in Gasow *et al.* (2021) is of order 10^{-7} . These values are still much larger than those of porous media in real applications.

An important motivation for microscopic simulations is to better understand the dynamics of turbulent eddies in porous media. This is crucial for predicting dissipation rates in both flow and temperature fields. According to the derivation by Jin and Herwig (2014), these dissipation rates determine both pressure drop and heat transfer rates. PSR-DNS and PSR-LES offer more accurate predictions of dissipation rates compared with RANS, since dissipation is either directly calculated (in PSR-DNS) or modeled with minimal assumptions (in PSR-LES). With a better grasp of the underlying physics, more precise modeling of turbulence transport in porous media becomes feasible.

A crucial fundamental question about the eddy dynamics in porous media is whether turbulence models should account only for turbulence structures limited in size to the pore scale or whether the size of turbulence structures could exceed the pore scale. The latter would imply the existence of macroscopic turbulence in porous media, where the turbulent eddies are larger than the size of the pores. To address this fundamental question, Jin *et al.* (2015) conducted a DNS study. Both transient and statistical results demonstrate that the length scales of turbulent structures are constrained by the pore size, thereby suggesting the pore-scale prevalence hypothesis (PSPH) when the porosity is not close to unity. Later, Uth *et al.* (2016) and Jin and Kuznetsov (2017) simulated turbulent flows in

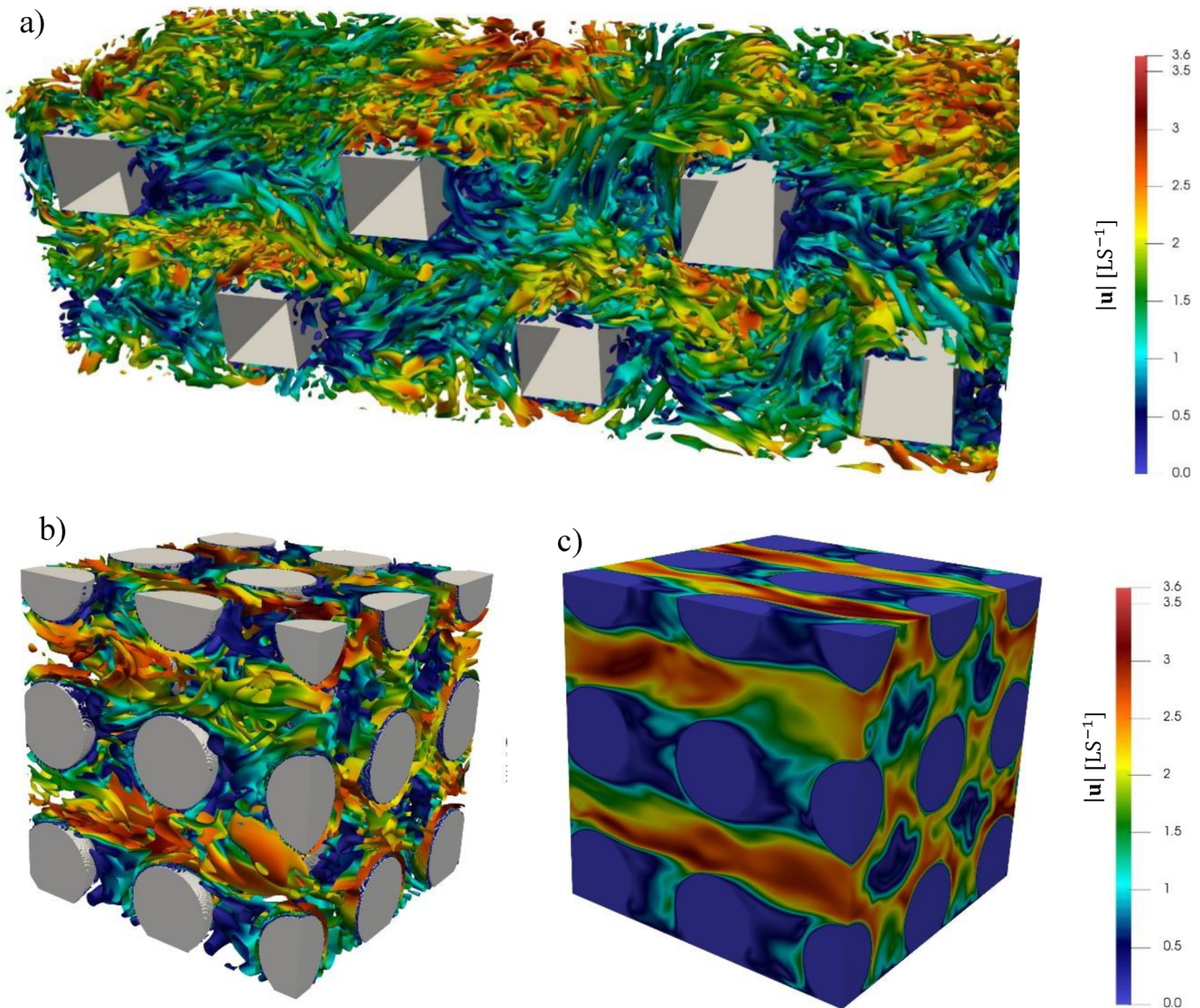


FIG. 2. Snapshots of turbulent flows in porous media obtained by post-processing of the DNS results of [Jin *et al.* \(2015\)](#) and [Jin and Kuznetsov \(2017\)](#). (a) Turbulent structures in a porous matrix composed of two-dimensional square cylinders, $Re_d = 750$. (b) Turbulent structures in a porous matrix composed of three-dimensional spheres, $Re_d = 500$. (c) Instantaneous velocity magnitude for flows in a porous matrix composed of three-dimensional spheres, $Re_d = 500$.

more complicated porous matrices. The DNS results further confirmed the PSPH. [Figure 2](#) shows snapshots of turbulent structures in porous media with different pore-scale geometries. The snapshots show qualitatively that the length scales of turbulence are limited by the pore size. [Rao and Jin \(2022\)](#) indicate that the macroscopic turbulence may survive when the porosity is larger than a critical value, which is in the range 0.93–0.98.

Some other DNS studies have investigated the interaction between a turbulent flow in porous media and a free turbulent flow. The computational domain is partly occupied by a porous medium. For example, [Motlagh and Taghizadeh \(2016\)](#) studied the transverse

pressure waves caused by the Kelvin–Helmholtz (K–H) instability over porous and rough walls. [Kuwata and Suga \(2016; 2017\)](#) studied turbulence over anisotropic porous walls. The arrays of porous elements are displayed systematically to introduce anisotropic permeability. The DNS results indicate that permeability in the streamwise (flow) and spanwise (cross-flow) directions enhances turbulence, while permeability in the wall-normal direction does not. Permeability has been shown to play a major role in determining the response of channel flow to permeable walls in DNS studies by [Rosti *et al.* \(2015, 2018\)](#), even if the permeability has a very small value. These studies also showed that making porous media anisotropic

could reduce drag across a permeable wall by about 20%. The DNS results by [Gómez-de-Segura and García-Mayoral \(2019\)](#) reveal a linear relationship between drag reduction and the difference between the streamwise and spanwise permeabilities when the permeability is small. This linear relationship holds when the wall-normal permeability normalized by the viscous length scale K_y^+ is above a critical value ($\sqrt{K_y^+} \geq 0.38$). Interpreting the DNS results with the transfer entropy concept, [Wang et al. \(2021; 2022\)](#) investigated the effects of permeability on the intensity, time scale, and spatial extent of surface–subsurface interactions. A neural network-based remote sensing model was used to validate the statistical results.

Flow and heat transfer in packed beds are also important topics for microscopic simulations. For example, [Hutter et al. \(2011\)](#) simulated flows in a periodic open-cell structure in the turbulent regime using LES. Pore-scale Reynolds numbers in the range between 1200 and 4500 were considered. [Shams et al. \(2014\)](#) performed an LES of flows in a randomly stacked bed composed of spherical pebbles with a Reynolds number of 9753. Since DNS is computationally very expensive at high Reynolds numbers, the flow at a high pore-scale Reynolds number can be simulated by using LES. [He et al. \(2018; 2019\)](#) performed DNS studies in a triply periodic unit cell of a face-centered cubic (FCC) lattice. The DNS results confirm the absence of macroscale turbulence structures for this configuration. In addition,

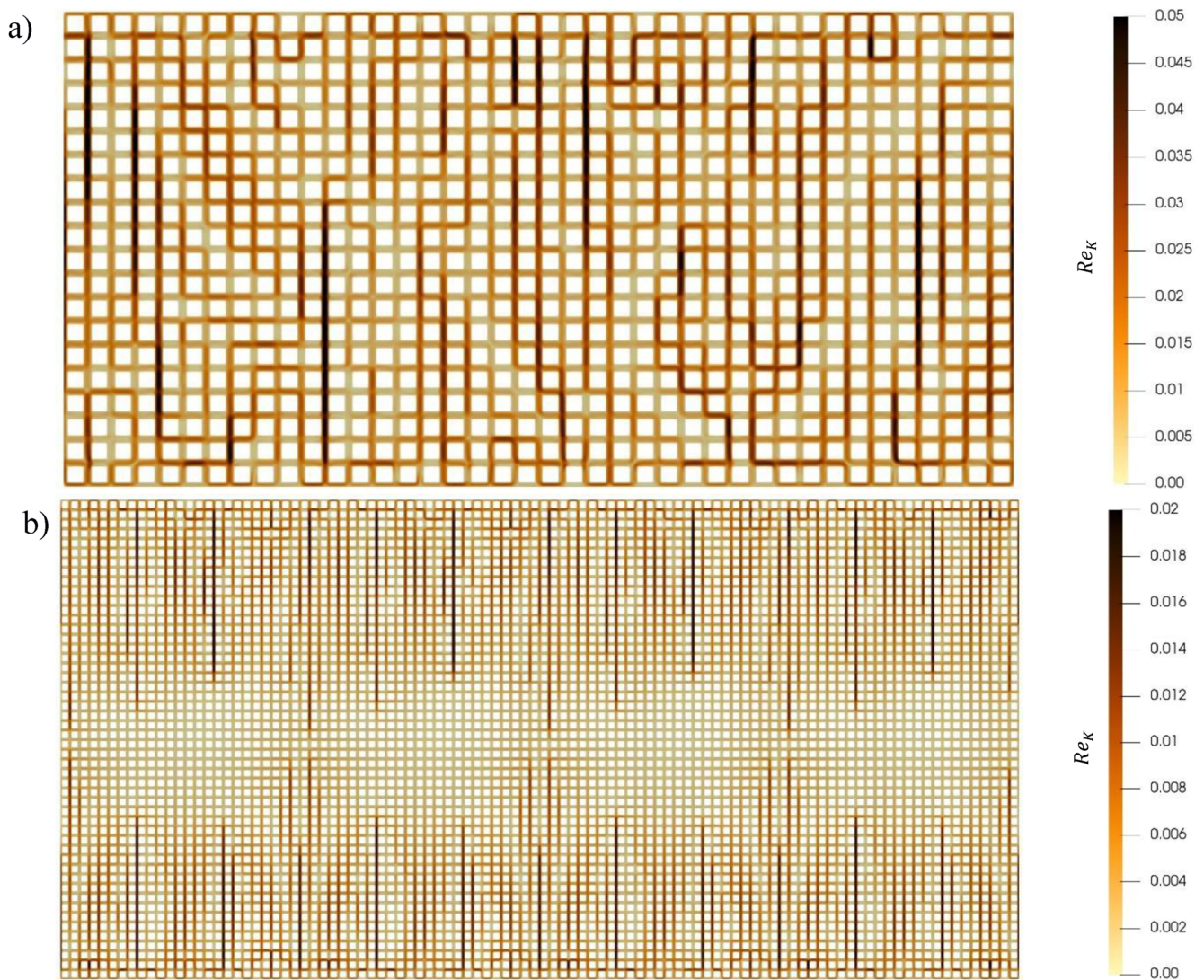


FIG. 3. Snapshots of local Reynolds number Re_k for natural convection in porous media: post-processing of the DNS results of [Gasow et al. \(2020; 2021\)](#). (a) $Ra = 20\,000$, $Da = 8.8 \times 10^{-6}$; (b) $Ra = 20\,000$, $Da = 4.4 \times 10^{-7}$.

the up-scaled flow statistics are well captured by the REV even if the flow in the pore is strongly anisotropic. Using both LES and DNS methods, [Srikanth et al. \(2021\)](#) studied the mechanism of a symmetry breaking phenomenon that occurs in turbulent flow in periodic porous media at a low value of porosity. The symmetry breakdown causes a deviation in the macroscale flow direction, which in turn introduces anisotropy in the macroscale Reynolds stress. Using LES, [Huang et al. \(2022\)](#) studied the effects of microscale vortices on convective heat transfer in turbulent flow within porous media. The numerical results show that both vortex shedding and secondary flow instabilities have significant influences on the Nusselt number. Local Nusselt number peaks coincided with the regions of flow mixing surrounding flow stagnation points on the solid obstacle surface. [Rao and Jin \(2022\)](#) simulated turbulent flows in a porous matrix characterized by two length scales using DNS. The DNS results indicate that macroscopic turbulence structures may survive when the porosity is very high. [Apte et al. \(2022\)](#) studied the clustering of inertial particles in turbulent flow through a porous unit cell. The DNS results show a large number of small volumes where cluster destruction is prominent. These small volumes are generated by the collision of particles with the wall surfaces of the porous elements.

Besides the conventional turbulent flows in porous media introduced above, it is also necessary to mention the pseudo-turbulence arising in natural convection in porous media. [Figure 3](#) shows snapshots of the instantaneous local Reynolds number Re_K , which is based on permeability K and local velocity magnitude $|\mathbf{u}|$. These flows are usually characterized by very low local Reynolds numbers, and so the Forchheimer term, which characterizes the contribution of the form drag, can be neglected. However, the flow exhibits chaotic behavior at a large Rayleigh number. Conventional turbulent flows do not exhibit this behavior. Intensive DNS studies have been carried out in recent years to understand pseudo-turbulence in porous media. For example, based on a microscopic simulation study, [Gasow et al. \(2020; 2021; and 2022\)](#) found that the effects of pore-scale motions on the macroscopic instabilities of natural convection cannot be neglected. [Liu et al. \(2020\)](#) found that the scaling of the Nusselt number vs Ra is significantly affected by the ratio of the pore scale to the thickness of the thermal boundary layer. [Korba and Li \(2022\)](#) studied the pore-scale effects on natural convection induced by conjugate heat transfer.

A significant real-world application of pseudo-turbulence in natural convection in porous media is the CO₂ sequestration process in deep saline aquifers ([Benson and Cole. 2008; Huppert and Neufeld, 2014](#)). However, the actual CO₂ sequestration process is considerably more complex than those examined in fundamental studies. One crucial aspect to consider is the influence of multiphase flows. First, the presence of different phases affects the flow dynamics in porous media owing to surface tension effects. Additionally, the permeability of the porous medium varies when multiple phases are involved. Despite the increasing attention paid to multiphase flows in porous media in recent years, as evidenced by studies such as those by [Gruener et al. \(2012\)](#), [Sun et al. \(2016\)](#), and [Li et al. \(2022\)](#), there remains a notable gap in research concerning turbulence (or pseudo-turbulence) in multiphase flows. In addition, the Darcy numbers used in the microscopic simulations are much higher than those in real applications. Calculations with lower Darcy numbers are required to provide better understanding of pseudo-turbulence in porous media.

III. MACROSCOPIC EQUATIONS FOR TURBULENT FLOWS IN POROUS MEDIA

A double-decomposition concept is often used for developing the macroscopic equations of turbulent flows in porous media. This is described in detail by [Pedras and de Lemos \(2000; 2001a; 2001b; 2001c; 2003\)](#); [de Lemos \(2012\)](#); [Rocamora and de Lemos \(2000\)](#); [de Lemos and Rocamora \(2002\)](#); [de Lemos and Braga \(2003\)](#); [de Lemos and Mesquita \(2003\)](#); and [de Lemos and Tofaneli \(2004\)](#). According to this concept, through time and volume averaging, any property φ can be decomposed as follows:

$$\varphi = \underbrace{\langle \bar{\varphi} \rangle^i}_{\langle \varphi \rangle^i} + \underbrace{\langle \varphi' \rangle^i}_{\langle \varphi' \rangle^i} + \overbrace{\bar{\varphi} + \langle \varphi' \rangle^i}^{\varphi} = \underbrace{\langle \varphi \rangle^i + \bar{\varphi}}_{\bar{\varphi}} + \underbrace{\langle \varphi' \rangle^i + \langle \varphi' \rangle^i}_{\langle \varphi' \rangle^i} \quad (4)$$

The overbar $\bar{\cdot}$ denotes time averaging and the angular brackets $\langle \cdot \rangle^i$ denote volume averaging over the fluid region of an REV. The operation $\bar{\varphi}$ is defined as $\bar{\varphi} = \varphi - \langle \varphi \rangle^i$. The different sequences of time and volume averaging result in two types of expressions; however, these are equivalent. In Eq. (4), $\langle \bar{\varphi} \rangle^i = \langle \varphi \rangle^i$ is the intrinsic average of the time-mean property, $\langle \varphi' \rangle^i = \langle \varphi \rangle^i$ is the intrinsic average of the property fluctuation, $\bar{\varphi} = \varphi - \langle \varphi \rangle^i$ is the spatial deviation of the mean property, and $\langle \varphi' \rangle^i$ is the spatial deviation of the property fluctuation.

If the time and volume averaging are performed for the incompressible Navier–Stokes equations (1) and (2), the following macroscopic equations are obtained:

$$\frac{\partial(\phi \langle \bar{u}_i \rangle^i)}{\partial x_i} = 0, \quad (5)$$

$$\begin{aligned} \frac{\partial(\phi \langle \bar{u}_i \rangle^i)}{\partial t} + \frac{\partial(\bar{R}_{ij}^I + \bar{R}_{ij}^{II} + \bar{R}_{ij}^{III} + \bar{R}_{ij}^{IV})}{\partial x_j} \\ = - \frac{\partial(\phi \langle \bar{p} \rangle^i)}{\partial x_i} + \nu \frac{\partial^2(\phi \langle \bar{u}_i \rangle^i)}{\partial x_j^2} + \phi g_i + \phi \bar{R}_i, \end{aligned} \quad (6)$$

where ϕ is the porosity, $\bar{R}_{ij}^I = \phi \langle \bar{u}_i \rangle^i \langle \bar{u}_j \rangle^i$ is the convective term of the macroscopic mean velocity, $\bar{R}_{ij}^{II} = \phi \langle \bar{u}_i \rangle^i \langle \bar{u}_j \rangle^i$ is the spatial dispersion of the microscopic mean velocity, $\bar{R}_{ij}^{III} = \phi \langle \bar{u}_i' \rangle^i \langle \bar{u}_j' \rangle^i$ are the turbulent Reynolds stresses due to the macroscopic velocity fluctuation, and $\bar{R}_{ij}^{IV} = \phi \langle \bar{u}_i' \rangle^i \langle \bar{u}_j' \rangle^i$ is the turbulent dispersion. Obviously, \bar{R}_{ij}^{II} , \bar{R}_{ij}^{III} , and \bar{R}_{ij}^{IV} , which have 18 unknown components, need to be modeled before the macroscopic governing equations can be solved. This procedure is called model closure. In addition, the time-averaged total drag term \bar{R}_i also needs to be modeled.

Some studies have obtained the macroscopic equations using only volume averaging, without adopting time averaging ([Quintard and Whitaker, 1993; Whitaker, 1996; 1999; Wood and Valdés-Parada, 2013; and Lasseux et al., 2019](#)). The governing equations for studying transient natural convection in porous media have also been obtained only using volume averaging ([Gasow et al., 2020](#);

2021; and 2022). The governing equations for macroscopic flows (without considering the buoyancy force) read

$$\frac{\partial(\phi\langle u_i \rangle^i)}{\partial x_i} = 0, \quad (7)$$

$$\frac{\partial(\phi\langle u_i \rangle^i)}{\partial t} + \frac{\partial(\hat{R}_{ij}^I + \hat{R}_{ij}^{II})}{\partial x_j} = -\frac{\partial(\phi\langle p \rangle^i)}{\partial x_i} + \nu \frac{\partial^2(\phi\langle u_i \rangle^i)}{\partial x_j^2} + \phi g_i + \phi \hat{R}_i, \quad (8)$$

where $\hat{R}_{ij}^I = \phi\langle u_i^i u_j \rangle^i$ is the convective term of the macroscopic velocity and $\hat{R}_{ij}^{II} = \phi\langle u_i^i u_j \rangle^i$ is the spatial dispersion term. Now, only six unknown variables in the convective term and the volume-averaged drag \hat{R}_i need to be modeled.

IV. CLOSURE OF MACROSCOPIC EQUATIONS

The modeling of the unknown terms in the macroscopic equations (5)–(8) has been extensively studied. Early studies focused on modeling the total drag, while turbulence in porous media has received little attention apart from its effect on the total drag. Some classical models for the total drag are still widely used in modern CFD simulations. We will start our discussion with these classical models, which will be introduced in Sec. IV A.

Modeling turbulence in porous media has received increasing attention in recent years. It has been reviewed in the paper by Wood *et al.* (2020), the books by de Lemos (2012) and Nield and Bejan (2017), and in many review chapters, such as those by Lage *et al.* (2002), de Lemos (2004; 2005), and Vafai (2005). In general, there are two distinct views on turbulence in porous media. The first class of models are called macroscopic turbulence models, which deal primarily with macroscopic turbulence in porous media. The second approach was originally expressed in Nield (1991) and then further developed in other studies, such as those by Nield (2001), Jin *et al.* (2015), Uth *et al.* (2016), and Jin and Kuznetsov (2017). According to the second approach, macroscopic turbulence is impossible owing to the pore-scale limitation on the size of turbulent eddies, at least in a dense porous medium. All turbulence models according to this view are microscopic turbulence models. Macroscopic turbulence models and microscopic turbulence models will be discussed in detail in Secs. IV B and IV C.

A. Total drag

The study of the total drag can be traced back to the classical experimental study of water filtration through columns of sand performed by Darcy in 1856 (Nield and Bejan, 2017). In his experiment, Darcy found a linear relationship between the superficial velocity and the pressure gradient for porous media flow problems characterized by low velocity. This linear relationship has been verified by many later experiments, leading to Darcy’s law. In the macroscopic momentum equation (6), the Darcy’s law is described as follows:

$$\bar{R}_i = \frac{\nu}{K} \bar{u}_{Di} = \frac{\nu}{K} \phi \langle \bar{u}_i \rangle^i, \quad (9)$$

where $\bar{u}_{Di} = \phi \langle \bar{u}_i \rangle^i$ is the superficial velocity and K is the permeability, which is determined by the pore-scale geometry. For a packed bed made of spheres or fibers, K can be estimated by using the

Carman–Kozeny equation (Kozeny, 1927; Carman, 1956), expressed as

$$K = \frac{D_{P2}^2 \phi^3}{180(1 - \phi)^2}, \quad (10)$$

where D_{P2} is an effective average particle or fiber diameter.

Darcy’s equation is only valid when the superficial velocity \bar{u}_{Di} is small. At high Reynolds numbers, Darcy’s law breaks down because the form drag caused by solid obstacles becomes comparable to the surface drag resulting from friction. When the Reynolds number Re_K based on the superficial velocity magnitude $|\bar{u}_D|$ and the pore size \sqrt{K} is larger than 1 but the flow is not yet turbulent, the Darcy equation should be replaced with the Darcy–Forchheimer equation, expressed as

$$\bar{R}_i = \frac{\nu}{K} \hat{u}_{Di} + \frac{c_F}{\sqrt{K}} |\bar{u}_D| \hat{u}_{Di}, \quad (11)$$

where c_F is a dimensionless coefficient that takes into account the nonlinear increase in drag with speed. Beavers *et al.* (1973) showed that c_F can be expressed as

$$c_F = 0.55 \left(1 - 5.5 \frac{d}{D_e} \right), \quad (12)$$

where d is the sphere diameter and D_e is the equivalent diameter of the bed. Masuoka and Takatsu (1996) and Wood *et al.* (2020) hypothesized that the Darcy–Forchheimer equation is valid for both laminar and turbulent flows. A similar approach was proposed by Zhu and Kuznetsov (2005), Kuznetsov (2004a, 2004b), Kuznetsov and Becker (2004), and Kuznetsov *et al.* (2002; 2003), in which turbulent flow in composite porous/fluid channels was simulated by using a turbulent model in the clear fluid region and the Darcy–Forchheimer model in the porous region of the channel. The solutions in the clear and porous regions were then matched at the interface. This approach was based on the hypothesis that in composite porous/fluid channels, even if the flow is turbulent in the fluid region, turbulence structures cannot penetrate deep into the porous region of the channel. As an alternative form of the Darcy–Forchheimer equation, Irmay (1958) suggested calculating the total drag as

$$\bar{R}_i = \frac{\beta(1 - \phi)^2}{D_{P2}^2 \phi^3} u_{Di} + \frac{\alpha(1 - \phi)}{D_{P2}^2 \phi^3} |\bar{u}_D| \bar{u}_{Di}, \quad (13)$$

which is also known as Ergun’s equation. The model coefficients α and β have values of 1.75 and 150, respectively.

However, later studies have shown that the Darcy–Forchheimer equation cannot fully describe the total drag of a turbulent flow in a porous medium. For example, Lage *et al.* (1997) indicated that c_F is not a constant but is related to the superficial (filtration) flow velocity. Rao *et al.* (2020) suggested the following Taylor expansion of \bar{R}_i with respect to a local Reynolds number Re_K :

$$\bar{R}_i = \frac{\nu}{K} u_{Di} \left[1 + c_{F1} Re_K + c_{F2} Re_K^2 + \dots + c_{Fn} Re_K^n + O(Re_K^{n+1}) \right], \quad (14)$$

where $c_{F1}, c_{F2}, \dots, c_{Fn}$ are the coefficients of the Taylor series. Re_K is the local Reynolds number based on the permeability, calculated as

$$Re_K = \frac{\sqrt{K}|\bar{\mathbf{u}}_D|}{\nu} \quad (15)$$

To determine the total drag of a turbulent flow in porous media, at least c_{F1} and c_{F2} should be taken into account.

Whitaker (1996) suggested a mathematical derivation of the Darcy–Forchheimer equation. The equation for a homogeneous porous medium is

$$\bar{\mathbf{u}}_D = -\frac{\mathbf{K}}{\mu} \cdot (\nabla \langle p \rangle^i - \rho \mathbf{g}) - \mathbf{F}(Re_p) \cdot \bar{\mathbf{u}}_D, \quad (16)$$

where \mathbf{K} is the permeability tensor and \mathbf{F} the Forchheimer correction tensor. Using an upscaling technique, Lasseux *et al.* (2019) also suggested a derivation of the macroscopic model for periodic porous media. They argued that a Darcy-like model with an accumulation term involving the derivative of the superficial velocity is inappropriate for unsteady flows.

A Laplacian term is often added to the macroscopic momentum equation to account for the effects of the mean velocity gradient, thus allowing for the imposition of boundary conditions at the domain walls and the interface; the latter applies to composite porous/fluid domains. Neglecting \bar{R}_{ij}^{II} , \bar{R}_{ij}^{III} , and \bar{R}_{ij}^{IV} , the time- and volume-averaged macroscopic momentum equation (6) becomes

$$\frac{\partial \bar{u}_{Di}}{\partial t} + \frac{\partial (\bar{u}_{Di} \bar{u}_{Di} / \phi)}{\partial x_j} = -\frac{\partial (\phi \langle P \rangle^i)}{\partial x_i} + \frac{\partial}{\partial x_j} \left(\bar{\nu} \frac{\partial \bar{u}_{Di}}{\partial x_j} \right) + \phi g_i + \phi \bar{R}. \quad (17)$$

The effective kinematic viscosity $\bar{\nu}$ was originally assumed to be identical to the molecular viscosity ν (Brinkman, 1949). However, later studies showed that $\bar{\nu}$ is larger than ν (Givler and Altobelli, 1994; Kuznetsov, 1997; Vafai, 2005; Ochoa-Tapia and Whitaker, 1995; Bear and Bachmat, 1990; Saez *et al.*, 1991; Vafai and Tien, 1981; 1982; Hsu and Cheng, 1990; Valdes-Parada *et al.*, 2007; and Auriault, 2009). Kuznetsov and Kuznetsov (2017) showed that the viscosity ratio $\bar{\nu}/\nu$ can be as large as 8. Nevertheless, some other studies have questioned the validity of the Brinkman equation (Durlafsky and Brady, 1987; Rubinstein, 1986; Gerritsen *et al.*, 2005; and Auriault, 2009). Nield and Bejan (2017) suggested that the Laplacian term is unnecessary since it only affects a thin layer. Therefore, it is still an open question whether the drag force due to the mean velocity gradient can be modeled by the Brinkman equation.

B. Macroscopic turbulence models

Information about turbulence transport is required in a macroscopic turbulence model. Lee and Howell (1991), Prescott and Incropera (1995), and Lage *et al.* (1997) reported representative models of this type. These macroscopic models are similar to turbulence models for clear fluid flows. The transport equations for turbulent kinetic energy and dissipation rate are often solved in these models. In addition, some turbulence models attempt to simulate both pore-scale and large-scale turbulence. Thus, macroscopic transport of turbulence is also accounted for in these models. Representative models are those developed by de Lemos and colleagues; see de Lemos and Braga (2003), de Lemos and Mesquita (2003), de Lemos and Pedras (2001), de Lemos and Rocamora (2002), de Lemos and Tofaneli (2004), Pedras and de Lemos (2000; 2001a; 2001b; 2001c; 2003), and Silva and de Lemos (2003).

To close the macroscopic equations, the tensors \bar{R}_{ij}^{II} , \bar{R}_{ij}^{III} , and \bar{R}_{ij}^{IV} for the time- and volume-averaged equations need to be modeled. It should be noted that even if the flow is not turbulent, the spatial dispersion of the microscopic mean velocity \bar{R}_{ij}^{II} still needs to be modeled when the mean velocity gradient is not zero. However, \bar{R}_{ij}^{II} has received very little attention in modern turbulence models.

When the flow is turbulent, Lage *et al.* (1997) suggested calculating the macroscopic Reynolds stress tensor $\bar{R}_{ij}^{III} + \bar{R}_{ij}^{IV} = \phi \langle u'_i u'_j \rangle^i$ as follows:

$$-\bar{R}_{ij}^{III} - \bar{R}_{ij}^{IV} = -\phi \overline{\langle u'_i u'_j \rangle^i} = 2\nu_{t\phi} s_{Dij} + \frac{2}{3} \phi \rho \langle k \rangle^i \delta_{ij}, \quad (18)$$

where $s_{Dij} = \frac{1}{2} \left(\frac{\partial \bar{u}_{Di}}{\partial x_j} + \frac{\partial \bar{u}_{Dj}}{\partial x_i} \right)$ is the macroscopic strain tensor and $\nu_{t\phi}$ is the turbulent viscosity. In macroscopic turbulence models, additional transport equations for the turbulence quantities [e.g., kinetic energy $\langle k \rangle^i$ and turbulence dissipation rate $\langle \varepsilon \rangle^i$] are solved to determine $\nu_{t\phi}$. For example, in a k – ε model, it is calculated as

$$\nu_{t\phi} = c_\mu \frac{\langle k \rangle^i}{\langle \varepsilon \rangle^i}. \quad (19)$$

The effective viscosity $\bar{\nu}$ is calculated as the sum of ν and $\nu_{t\phi}$. There are different versions of the transport equations for $\langle k \rangle^i$ and $\langle \varepsilon \rangle^i$. For example, Pedras and de Lemos (2000; 2001a; 2001b; and 2001c) suggested the following equations:

$$\frac{\partial (\phi \langle k \rangle^i)}{\partial t} + \frac{\partial (\bar{u}_{Di} \langle k \rangle^i)}{\partial x_i} = \frac{\partial}{\partial x_j} \left(\bar{\nu} \frac{\partial (\phi \langle k \rangle^i)}{\partial x_j} \right) - \phi \overline{\langle u'_i u'_j \rangle^i} \frac{\partial (\bar{u}_{Di})}{\partial x_i} + c_k \phi \frac{\langle k \rangle^i |\bar{\mathbf{u}}_D|}{\sqrt{K}} - \phi \langle \varepsilon \rangle^i, \quad (20)$$

and

$$\frac{\partial (\phi \langle \varepsilon \rangle^i)}{\partial t} + \frac{\partial (\bar{u}_{Di} \langle \varepsilon \rangle^i)}{\partial x_i} = \frac{\partial}{\partial x_j} \left(\bar{\nu} \frac{\partial (\phi \langle \varepsilon \rangle^i)}{\partial x_j} \right) - c_{1\varepsilon} \phi \overline{\langle u'_i u'_j \rangle^i} \frac{\partial (\bar{u}_{Di})}{\partial x_i} \times \frac{\langle \varepsilon \rangle^i}{\langle k \rangle^i} + c_{2\varepsilon} \phi \left(\frac{\langle \varepsilon \rangle^i |\bar{\mathbf{u}}_D|}{\sqrt{K}} - \frac{\langle \varepsilon \rangle^i}{\langle k \rangle^i} \right). \quad (21)$$

In a more recent study, Nakayama and Kuwahara (2008) proposed the following transport equations:

$$\frac{\partial (\langle k \rangle^i)}{\partial t} + \frac{\partial (\bar{u}_i \langle k \rangle^i)}{\partial x_i} = \frac{\partial}{\partial x_j} \left[\left(\nu + \frac{\nu_{t\phi}}{\sigma_k} \right) \delta_{ij} + \frac{(a_{dis})_{ij}}{Le_k \phi} \right] \frac{\partial (\langle k \rangle^i)}{\partial x_j} - 2\nu_{t\phi} \langle s_{ij} \rangle^i \langle s_{ij} \rangle^i + \phi^2 (b \langle \bar{u}_i \rangle^i \langle \bar{u}_i \rangle^i)^{3/2} - \langle \varepsilon \rangle^i, \quad (22)$$

and

$$\frac{\partial (\langle \varepsilon \rangle^i)}{\partial t} + \frac{\partial (\bar{u}_i \langle \varepsilon \rangle^i)}{\partial x_i} = \frac{\partial}{\partial x_j} \left[\left(\nu + \frac{\nu_{t\phi}}{\sigma_\varepsilon} \right) \delta_{ij} + \frac{(a_{dis})_{ij}}{Le_\varepsilon \phi} \right] \frac{\partial (\langle \varepsilon \rangle^i)}{\partial x_j} - 2c_1 \nu_{t\phi} \langle s_{ij} \rangle^i \langle s_{ij} \rangle^i + c_2 \phi^2 b \sqrt{\frac{c_D \phi}{2K}} \times (\langle \bar{u}_i \rangle^i \langle \bar{u}_i \rangle^i)^2 - c_2 \frac{\langle \varepsilon \rangle^i}{\langle k \rangle^i}, \quad (23)$$

where $(a_{dis})_{ij}$ are the components of the thermal diffusivity tensor. Le_k and Le_ε are the Lewis numbers for mechanical dispersion

of the turbulence kinetic energy and dissipation rate, respectively, both of which are believed to be close to unity. The turbulence model developed by Nakayama and Kuwahara (2008) is obtained by volume averaging the transport equations for k and ϵ , while that developed by Pedras and de Lemos (2000) is obtained by averaging the transport equations in the fluid phase. In addition, the two models different in their source terms.

Macroscopic turbulence models have been widely applied to the solution of many engineering problems. For example, they have been applied to the study of flows in packed beds, in channels, in pipes, and in bundles of rods (Nakayama and Kuwahara, 2008). They have also been used in the simulation of flow in a porous matrix, which is a periodic array of square cylinders (Kazerooni and Hannani, 2009; Kundu et al., 2014). The macroscopic models have a common characteristic, namely, the transport of macroscopic turbulence in porous media is simulated in these models.

C. Microscopic turbulence models

Besides the macroscopic models for the simulation of turbulence in porous media, there are other types of turbulence models, namely, microscopic turbulence models. In microscopic turbulence models, the effect of turbulence can be accounted for by the source terms in the momentum and energy equations. Thus, it is not necessary to calculate the transport of turbulence. These types of turbulence models originate from Nield (1991). The models developed by Nakayama and Kuwahara (1999) and Kuwahara et al. (1998) also belong to the class of microscopic turbulence models.

Later, Jin et al. (2015), Uth et al. (2016), and Jin and Kuznetsov (2017) carried out systematic DNS studies to understand turbulence in porous media. Porous matrices composed of two-dimensional square and circular cylinders, three-dimensional spheres unbounded or bounded by walls, and a three-dimensional matrix with two characteristic pore scales have been investigated. The DNS results obtained suggest that the size of turbulent vortices is limited by the pore size, leading to the proposition of the pore-scale prevalence hypothesis (PSPH).

On the basis of the PSPH, Rao et al. (2020) proposed a microscopic turbulence model. In this model, it is assumed that turbulence production and dissipation are in equilibrium, and so it is not necessary to account for the transport of turbulence quantities. The effects of turbulence on momentum transport are accounted for by a symmetric tensor $D_{ij} = 2\bar{v}s_{Dij}$, where \bar{v} is an effective viscosity. Thus, the macroscopic momentum equation reads

$$\frac{\partial \bar{u}_{Di}}{\partial t} + \frac{\partial (\bar{u}_{Di}\bar{u}_{Di}/\phi)}{\partial x_j} = -\frac{1}{\rho} \frac{\partial (\phi(p)^i)}{\partial x_i} + \phi g_i - \phi \bar{R}_i + \frac{\partial D_{ij}}{\partial x_j}. \quad (24)$$

Characteristic length and velocity scales are needed to determine the effective viscosity \bar{v} . According to the PSPH, the flow in a porous medium is limited by the pore size s , which is used as a characteristic length scale. Here, \sqrt{K} is used to characterize the pore size s , because \sqrt{K} is proportional to s . However, unlike s or d , K can be determined even for a porous matrix with a complicated geometry. Similarly to the classical mixing length model for turbulent flows, the characteristic velocity is calculated as

$$\vartheta = \sqrt{K}|\bar{s}_{Dij}|, \quad (25)$$

where $|\bar{s}_{Dij}| = (2\bar{s}_{Dij}\bar{s}_{Dij})^{1/2}$ is the magnitude of the macroscopic strain rate. With the characteristic length scale \sqrt{K} and velocity scale ϑ , a local Reynolds number that represents the ratio between the inertial force and Darcy's force can be defined as

$$Re_d = \frac{K|\bar{s}_{Dij}|}{\nu}. \quad (26)$$

Then, a Taylor expansion of \bar{v}/ν with respect to Re_d leads to the following:

$$\bar{v}/\nu = c_{B1} + c_{B2}Re_d + \dots + c_{Bn}Re_d^{n-1} + O(Re_d^n), \quad (27)$$

where $c_{B1}, c_{B2}, \dots, c_{Bn}$ are the coefficients of the Taylor series. The following relations can be used to calculate c_{B1} and c_{B2} :

$$c_{B1} = 49.63 \times \frac{(1-\phi)^2}{\phi^{0.5}} + 1, \quad (28)$$

$$c_{B2} = 0.79 \times \frac{(1-\phi)^2}{\phi^3}. \quad (29)$$

More details about this microscopic model can be found in Rao et al. (2020). Although this model was proposed for the time- and volume-averaged Navier–Stokes equations, it is expected that a similar set of equations can be used as the volume-averaged Navier–Stokes equations (without time averaging):

$$\frac{\partial \hat{u}_{Di}}{\partial x_j} = 0, \quad (30)$$

$$\frac{\partial \hat{u}_{Di}}{\partial t} + \frac{\partial (\hat{u}_{Di}\hat{u}_{Di}/\phi)}{\partial x_j} = -\frac{1}{\rho} \frac{\partial (\phi(p)^i)}{\partial x_i} + \phi g_i - \phi \hat{R}_i + \frac{\partial}{\partial x_j} \left(\hat{v} \frac{\partial \hat{u}_{Di}}{\partial x_j} \right). \quad (31)$$

According to Eq. (31), turbulent motions are dampened by the total drag \hat{R}_i and the macroscopic diffusion $\frac{\partial}{\partial x_j} \left(\hat{v} \frac{\partial \hat{u}_{Di}}{\partial x_j} \right)$. However, macroscopic turbulence might survive if the total drag and the macroscopic diffusion are not strong enough to dampen all macroscopic instabilities.

Natural convection in porous media is usually simulated by solving the Darcy–Oberbeck–Boussinesq (DOB) equations. These are an alternative form of the macroscopic equations (30) and (31) (Nield and Bejan, 2017). The macroscopic instabilities in natural convection are induced by a buoyancy force, which is usually modeled with the Boussinesq hypothesis. Based on the volume-averaged Navier–Stokes equations (30) and (31), Gasow et al. (2021) developed a two-length-scale diffusion (TSLD) model for macroscopic simulations. In contrast to the DOB model, macroscopic diffusion is accounted for in the TSLD model. Numerical studies have shown that the macroscopic instabilities of natural convection in porous media can be accurately simulated by the volume-averaged equations (Hewitt et al., 2012; 2013; 2014; Wen et al., 2015; De Paoli et al., 2016¹⁷; Kränzien and Jin, 2019; Pirozzoli et al., 2021; and Gasow et al., 2021; 2022).

Figure 4 shows a snapshot of the local Reynolds number Re_K obtained from a macroscopic simulation with the TSLD model. Structures made of small proto-plumes near the walls and large

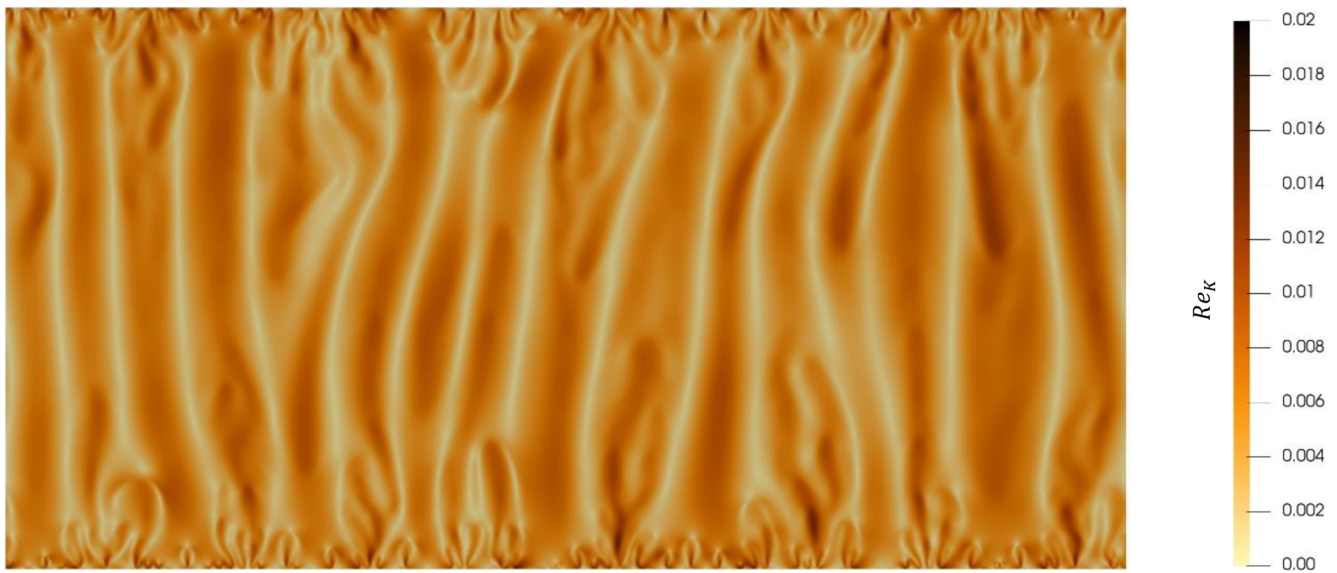


FIG. 4. Snapshot of the local Reynolds number Re_K for natural convection in porous media: post-processing of the macroscopic simulation results of Gasow *et al.* (2021), $Ra = 20\,000$, $Da = 4.4 \times 10^{-7}$.

mega-plumes near the domain center can be observed. The macroscopic and DNS results have been compared in Gasow *et al.* (2021; 2022). However, natural convection in porous media at high Rayleigh numbers has only macroscopic instabilities. There is no microscopic turbulence, owing to the low local Reynolds number. In this respect, the macroscopic instability for natural convection in porous media is called pseudo-turbulence, which is different from conventional turbulence.

Similar to classical turbulence, pseudo-turbulence is transient, chaotic, and random. However, whether pseudo-turbulence qualifies as real turbulence remains an open question. It is still unclear whether pseudo-turbulence follows the same energy cascade pattern as classical turbulent flows, which decay with a $5/3$ scaling at large Rayleigh numbers. Answering this question is crucial to determine the potential occurrence of macroscopic turbulence. Additionally, investigating whether the volume-averaged Eqs. (30) and (31) can accurately predict conventional macroscopic turbulence should be a focus of future research.

V. CONCLUSIONS AND OUTLOOK

With the rapid development of high-performance computers, CFD methods are becoming an efficient tool for analyzing and predicting turbulent flows in porous media. Microscopic simulations, including pore-scale-resolved DNS and LES, have considerably improved the understanding of turbulent flows in porous media, because they provide extensive flow details, including flow details in the pores.

In the past few years, the most active microscopic simulation studies of flows in porous media have focused on the pore-scale turbulent structures, turbulence length/time scales, turbulence at the interface of a porous medium and a clear flow region, and effects of

turbulence on heat/mass transfer. These studies have provided valuable knowledge for developing more efficient and accurate models for macroscopic simulations.

With time and volume averaging, or sometimes only volume averaging, the macroscopic equations for flows in porous media can be derived. It is more efficient to calculate the flows in porous media by solving the macroscopic equations; the corresponding simulations are called macroscopic simulations. Turbulence models for macroscopic simulations can be classified as macroscopic turbulence models, in which the macroscopic turbulence is simulated, or microscopic turbulence models, in which turbulence is simulated from direct solutions of the Navier–Stokes equations. DNS simulations performed by the present authors and their colleagues suggest that the pore scale limits the size of turbulent structures in porous media, unless the porosity is very large. With the new understanding of flow physics, new turbulence models for flows in porous media have emerged, including a microscopic turbulence model based on the PSPH.

Despite these advances, macroscopic modeling of turbulent flows in porous media is still a challenging task because of the complexity of the problem. Microscopic (DNS or LES) simulations are an important tool for reaching this target. Through microscopic simulations, the following fundamental questions need to be answered, which are key to developing more accurate and efficient macroscopic models:

1. How should the transport of macroscopic turbulence in porous media be modeled when it occurs? Although the DNS studies that have been conducted show no macroscopic turbulence unless the porosity is very high, there is evidence that macroscopic turbulence can occur at very large Reynolds numbers and high porosity values. In addition, it is important to know whether the pseudo-turbulence arising in natural convection in porous media is real turbulence.

2. What are the characteristics of turbulence at very high Reynolds numbers? The typical pore-scale Reynolds numbers in current DNS studies are of the order of $O(10^3)$. However, the pore-scale Reynolds numbers for nuclear pebble reactors can reach the order of $O(10^5)$. DNS studies of such problems are far beyond the capabilities of current high-performance computers. Whether turbulent flows at extremely high Reynolds numbers have new characteristics remains a mystery.
3. How does turbulence transport occur in inhomogeneous and anisotropic porous media? Turbulence in inhomogeneous and anisotropic porous media has different length/time scales. How motions with different length/time scales interact with each other is still unknown. A specific situation is the flow in a domain partly occupied by a porous medium and partly by a clear fluid. Modeling turbulent flow in inhomogeneous and anisotropic porous media remains a challenging task.
4. How does compressibility affect turbulent flows in porous media? Compressibility of the fluid in porous media flows has yet to be considered, partly because most previous studies have considered relatively low flow velocities. However, even if the Mach number in a porous medium is not very high, fluid compressibility still might have important effects when the temperature or pressure has strong variations. At present, very little is known about compressible flows in porous media.
5. How does turbulence or pseudo-turbulence occur, and how are the turbulence kinetic energy and thermal energy transported in multiphase flow? It is particularly important to understand how surface tension and variations in permeability caused by different phases affect turbulent flow in porous media.
6. How should fluid–structure interactions in porous media be modeled and simulated? Porous matrices may become deformable at very large Reynolds numbers. The ways in which turbulent flows interact with deformable structures should be investigated in greater depth in the future.

ACKNOWLEDGMENTS

The authors gratefully acknowledge the support for this study by the Deutsche Forschungsgemeinschaft (DFG, Grant Nos. 408356608 and 262377115). A.V.K. acknowledges the support of the National Science Foundation (Award No. CBET-2042834) and the Alexander Humboldt Foundation Research Award.

AUTHOR DECLARATIONS

Conflict of Interest

The authors have no conflicts to disclose.

Author Contributions

Yan Jin: Conceptualization (equal); Data curation (lead); Funding acquisition (equal); Methodology (equal); Project administration (equal); Writing – original draft (equal); Writing – review & editing (equal). **Andrey V. Kuznetsov:** Conceptualization (equal); Funding acquisition (equal); Investigation (equal); Methodology (equal);

Project administration (equal); Writing – original draft (equal); Writing – review & editing (equal).

DATA AVAILABILITY

The data that support the findings of this study are available from the corresponding author upon reasonable request.

REFERENCES

- Apte, S., Oujia T., Matsuda K., Kadoch B., He X., and Schneider K., “Clustering of inertial particles in turbulent flow through a porous unit cell,” *J. Fluid Mech.* **937**, A9 (2022).
- Auriault, J. L., “On the domain of validity of Brinkman’s equation,” *Transp. Porous Media* **79**, 215–223 (2009).
- Bear, J. and Bachmat Y., *Introduction to Modeling of Transport Phenomena in Porous Media* (Kluwer Academic, Dordrecht, 1990).
- Beavers, G. S., Sparrow E. M., and Rodenz D. E., “Influence of bed size on the flow characteristics and porosity of randomly packed beds of spheres,” *J. Appl. Mech.* **40**(3), 655–660 (1973).
- Belcher, S. E., “Mixing and transport in urban areas,” *Philos. Trans. R. Soc., A* **363**, 2947–2968 (2005).
- Belcher, S. E., Harman I. N., and Finnigan J. J., “The wind in the willows: Flows in forest canopies in complex terrain,” *Annu. Rev. Fluid Mech.* **44**, 479–504 (2012).
- Benson, S. M. and Cole D. R., “CO₂ sequestration in deep sedimentary formations,” *Elements* **4**(5), 325–331 (2008).
- Brinkman, H. C., “A calculation of the viscous force exerted by a flowing fluid on a dense swarm of particles,” *Flow, Turbul. Combust.* **1**, 27–34 (1949).
- Carman, P. C., *Flow of Gases Through Porous Media* (Butterworths, London, 1956).
- Chandesris, M., D’Hueppe, A., Mathieu, B., Jamet, D., and Goyeau, B., “Direct numerical simulation of turbulent heat transfer in a fluid-porous domain,” *Phys. Fluids* **25**, 125110 (2013).
- Chu, X., Yang, G., Pandey, S., and Weigand, B., “Direct numerical simulation of convective heat transfer in porous media,” *Int. J. Heat Mass Transfer* **133**, 11–20 (2019).
- Dave, A., Sun K., and Hu L., “Numerical simulations of molten salt pebble-bed lattices,” *Ann. Nucl. Energy* **112**, 400–410 (2018).
- de Lemos, M. J. S., “Turbulent heat and mass transfer in porous media,” in *Technologies and Techniques in Porous Media*, edited by Ingham, D. B., Bejan, A., Mamut, E., and Pop, I. (Kluwer Academic, Dordrecht, 2004), pp. 157–168.
- de Lemos, M. J. S., “The double-decomposition concept for turbulent transport in porous media,” in *Transport Phenomena in Porous Media III*, edited by Ingham, D. B. and Pop, I. (Elsevier, Oxford, 2005), pp. 1–33.
- de Lemos, M. J. S., *Turbulence in Porous Media, Modeling and Applications*, 2nd ed. (Elsevier, Oxford, UK, 2012).
- de Lemos, M. J. S. and Braga E. J., “Modeling of turbulent natural convection in porous media,” *Int. Commun. Heat Mass Transfer* **30**, 615–624 (2003).
- de Lemos, M. J. S. and Mesquita M. S., “Modeling of turbulent natural convection in porous media,” *Int. Commun. Heat Mass Transfer* **30**, 105–113 (2003).
- de Lemos, M. J. S. and Pedras M. H. J., “Recent mathematical models for turbulent flow in saturated rigid porous media,” *J. Fluids Eng.* **123**, 935–940 (2001).
- de Lemos, M. J. S. and Rocamora F. D., “Turbulent transport modeling for heat flow in rigid porous media,” in *Heat Transfer 2002 Proceedings of the 12th International Heat Transfer Conference* (Elsevier, 2002), Vol. 2, pp. 791–796.
- de Lemos, M. J. S. and Tofaneli L. A., “Modeling of double-diffusive turbulent natural convection in porous media,” *Int. J. Heat Mass Transfer* **47**, 4233–4241 (2004).
- De Paoli, M., Zonta, F., and Soldati, A., “Influence of anisotropic permeability on convection in porous media: Implications for geological CO₂ sequestration,” *Phys. Fluids* **28**, 056601 (2016).

- Diao, Z., Chen Z., Liu H., Wei B., and Hou J., "Pore-scale modeling of gravity-driven superheated vapor flooding process in porous media using the lattice Boltzmann method," *Int. Commun. Heat Mass Transfer* **146**, 106937 (2023).
- Durlafsky, L. and Brady J. F., "Analysis of the Brinkman equation as a model for flow in porous media," *Phys. Fluids* **30**, 3329–3341 (1987).
- Engineering Sciences Data Unit, "Low-fin staggered tube banks: Heat transfer and pressure drop for turbulent single phase cross flow," ESDU Data Item No. 84016, London, 1984.
- Ferdos, F. and Dargahi B., "A study of turbulent flow in large-scale porous media at high Reynolds numbers. Part I: Numerical validation," *J. Hydraul. Res.* **54**, 663–677 (2016).
- Gasow, S., Kuznetsov A. V., Avila M., and Jin Y., "A macroscopic two-length-scale model for natural convection in porous media driven by a species-concentration gradient," *J. Fluid Mech.* **926**, A8 (2021).
- Gasow, S., Kuznetsov, A. V., and Jin, Y., "Prediction of pore-scale-property dependent natural convection in porous media at high Rayleigh numbers," *Int. J. Therm. Sci.* **179**, 107635 (2022).
- Gasow, S., Lin Z., Zhang H. C., Kuznetsov A. V., Avila M., and Jin Y., "Effects of pore scale on the macroscopic properties of natural convection in porous media," *J. Fluid Mech.* **891**, A25 (2020).
- Gbadamosi, A. O., Junin R., Manan M. A., Agi A., and Yusuff A. S., "An overview of chemical enhanced oil recovery: Recent advances and prospects," *Int. Nano Lett.* **9**(3), 171–202 (2019).
- Gerritsen, M. G., Chen T., and Chen Q., personal communication, Stanford University, CA, 2005.
- Ghisalberti, M. and Nepf H., "Shallow flows over a permeable medium: The hydrodynamics of submerged aquatic canopies," *Transp. Porous Media* **78**, 385 (2009).
- Ghoreishi-Madiseh, S. A., Hassani F. P., Mohammadian A., and Radziszewski P. H., "A transient natural convection heat transfer model for geothermal borehole heat exchangers," *J. Renewable Sustainable Energy* **5**(4), 043104 (2013).
- Givler, R. C. and Altobelli S., "A determination of the effective viscosity for the Brinkman-Forchheimer flow model," *J. Fluid Mech.* **258**, 355–370 (1994).
- Gómez-de-Segura, G. and Garcia-Mayoral R., "Turbulent drag reduction by anisotropic permeable substrates – analysis and direct numerical simulations," *J. Fluid Mech.* **875**, 124–172 (2019).
- Gruener, S., Sadjadi Z., Hermes H. E., Kityk A. V., Knorr K., Egelhaaf S. U., Rieger H., and Huber P., "Anomalous front broadening during spontaneous imbibition in a matrix with elongated pores," *Proc. Natl. Acad. Sci. U.S.A.* **109**(26), 10245–10250 (2012).
- He, X., Apte S., Schneider K., and Kadoch B., "Angular multiscale statistics of turbulence in a porous bed," *Phys. Rev. Fluids* **3**(8), 084501 (2018).
- He, X., Apte S. V., Finn J. R., and Wood B. D., "Characteristics of turbulence in a face-centered cubic porous unit cell," *J. Fluid Mech.* **873**, 608–645 (2019).
- Hewitt, D. R., Neufeld J. A., and Lister J. R., "Ultimate regime of high Rayleigh number convection in a porous medium," *Phys. Rev. Lett.* **108**, 224503 (2012).
- Hewitt, D. R., Neufeld J. A., and Lister J. R., "Convective shutdown in a porous medium at high Rayleigh number," *J. Fluid Mech.* **719**, 551 (2013).
- Hewitt, D. R., Neufeld J. A., and Lister J. R., "High Rayleigh number convection in a three-dimensional porous medium," *J. Fluid Mech.* **748**, 879 (2014).
- Hsu, C. T. and Cheng P., "Thermal dispersion in a porous medium," *Int. J. Heat Mass Transfer* **33**, 1587–1597 (1990).
- Huang, C.-W., Srikanth V., and Kuznetsov A. V., "The evolution of turbulent micro-vortices and their effect on convection heat transfer in porous media," *J. Fluid Mech.* **942**, A16 (2022).
- Huppert, H. E. and Neufeld J. A., "The fluid mechanics of carbon dioxide sequestration," *Annu. Rev. Fluid Mech.* **46**, 255–272 (2014).
- Hutter, C., Zenklusen A., Kuhn S., and Rudolf von Rohr P., "Large eddy simulation of flow through a streamwise-periodic structure," *Chem. Eng. Sci.* **66**, 519–529 (2011).
- Irmay, S., "On the theoretical derivation of Darcy and Forchheimer formulas," *Trans., Am. Geophys. Union* **39**(4), 702–707 (1958).
- Jin, Y. and Herwig H., "Turbulent flow and heat transfer in channels with shark skin surfaces: Entropy generation and its physical significance," *Int. J. Heat Mass Transfer* **70**, 10–22 (2014).
- Jin, Y. and Herwig H., "Turbulent flow in rough wall channels: Validation of RANS models," *Comput. Fluids* **122**, 34–46 (2015).
- Jin, Y. and Kuznetsov A. V., "Turbulence modeling for flows in wall bounded porous media: An analysis based on direct numerical simulations," *Phys. Fluids* **29**, 045102 (2017).
- Jin, Y., Uth M.-F., Kuznetsov A. V., and Herwig H., "Numerical investigation of the possibility of macroscopic turbulence in porous media: A direct numerical simulation study," *J. Fluid Mech.* **766**, 76–103 (2015).
- Kazerooni, R. B. and Hannani, S. K., "Simulation of turbulent flow through porous media employing a v2f model," *Sci. Iranica Trans. B Mech. Eng* **16**, 159–167 (2009).
- Korba, D. and Li, L., "Effects of pore scale and conjugate heat transfer on thermal convection in porous media," *J. Fluid Mech.* **944**, A28 (2022).
- Kozeny, J., "Ueber kapillare Leitung des Wassers im Boden," *Sitzb. Akad. Wiss. Wien. Math. naturw. Klasse.* **136**(2a), 271–306 (1927).
- Kränzien, P. U. and Jin Y., "Natural convection in a two-dimensional cell filled with a porous medium: A direct numerical simulation study," *Heat Transfer Eng.* **40**, 487–496 (2019).
- Kundu, P., Kumar V., and Mishra I. M., "Numerical modeling of turbulent flow through isotropic porous media," *Int. J. Heat Mass Transfer* **75**, 40–57 (2014).
- Kuwata, Y. and Suga K., "Lattice Boltzmann direct numerical simulation of interface turbulence over porous and rough walls," *Int. J. Heat Fluid Flow* **61**, 145–157 (2016).
- Kuwata, Y. and Suga K., "Direct numerical simulation of turbulence over anisotropic porous media," *J. Fluid Mech.* **831**, 41–71 (2017).
- Kuznetsov, A. V., "Influence of the stress jump condition at the porous-medium/clear-fluid interface on a flow at a porous wall," *Int. Commun. Heat Mass Transfer* **24**, 401–410 (1997).
- Kuznetsov, A. V., "Effect of turbulence on forced convection in a composite tube partly filled with a porous medium," *J. Porous Media* **7**(1), 59–64 (2004a).
- Kuznetsov, A. V., "Numerical modeling of turbulent flow in a composite porous/fluid duct utilizing a two-layer $k-\epsilon$ model to account for interface roughness," *Int. J. Therm. Sci.* **43**, 1047–1056 (2004b).
- Kuznetsov, A. V. and Becker S. M., "Effect of the interface roughness on turbulent convective heat transfer in a composite porous/fluid duct," *Int. Commun. Heat Mass Transfer* **31**, 11–20 (2004).
- Kuznetsov, A. V., Cheng L., and Xiong M., "Effects of thermal dispersion and turbulence on forced convection in a composite parallel-plate channel: Investigation of constant wall heat flux and constant wall temperature cases," *Numer. Heat Transfer, Part A* **42**, 365–383 (2002).
- Kuznetsov, A. V., Cheng L., and Xiong M., "Investigation of turbulence effects on forced convection in a composite porous/fluid duct: Constant wall flux and constant wall temperature cases," *Heat Mass Transfer* **39**, 613–623 (2003).
- Kuznetsov, I. A. and Kuznetsov A. V., "Using resampling residuals for estimating confidence intervals of the effective viscosity and Forchheimer coefficient," *Transp. Porous Media* **119**, 451–459 (2017).
- Kuwahara, F., Kameyama, Y., Yamashita, S., and Nakayama, A., "Numerical modeling of turbulent flow in porous media using a spatially periodic array," *J. Porous Media* **1**, 47–55 (1998).
- Lage, J. L., Antohe B. V., and Nield D. A., "Two types of nonlinear pressure-drop versus flow-rate relation observed for saturated porous media," *J. Fluids Eng.* **119**(3), 700–706 (1997).
- Lage, J. L., de Lemos, M. J. S. and Nield, D. A., "Modeling turbulence in porous media," in *Transport Phenomena in Porous Media II*, edited by Ingham, D. B. and Pop, I. (Elsevier, Oxford, 2002), pp. 198–230.
- Lasseux, D., Valdés-Parada F. J., and Bellet F., "Macroscopic model for unsteady flow in porous media," *J. Fluid Mech.* **862**, 283–311 (2019).
- Lee, K.-B. and Howell J. R., "Theoretical and experimental heat and mass transfer in highly porous media," *Int. J. Heat Mass Transfer* **34**, 2123–2132 (1991).
- Li, S., Liu H., Wu R., Cai J., Xi G., and Jiang F., "Prediction of spontaneous imbibition with gravity in porous media micromodels," *J. Fluid Mech.* **952**, A9 (2022).

- Liu, S., Jiang L., Chong K. L., Zhu X., Wan Z. H., Verzicco R., Stevens R. J. A. M., Lohse D., and Sun C., "From Rayleigh-Bénard convection to porous-media convection: How porosity affects heat transfer and flow structure," *J. Fluid Mech.* **895**, A18 (2020).
- Liu, H., Sun S., Wu R., Wei B., and Hou J., "Pore-scale modeling of spontaneous imbibition in porous media using the lattice Boltzmann method," *Water Resour. Res.* **57**, e2020WR029219, (2021).
- Liu, W., Shi L., and Liu H., "Numerical study of the impact of geometrical parameters on the rarefied gas transport in porous media," *Gas Sci. Eng.* **110**, 204855 (2023).
- Lucci, F., Della Torre A., Montenegro G., Kaufmann R., and Dimopoulos Eggen-schwiler P., "Comparison of geometrical, momentum and mass transfer characteristics of real foams to Kelvin cell lattices for catalyst applications," *Int. J. Heat Mass Transfer* **108**, 341–350 (2017).
- Masouka, T. and Takatsu Y., "Turbulence model for flow through porous media," *Int. J. Heat Mass Transfer* **39**, 2803–2809 (1996).
- Meroney, R. N., "Fires in porous media: Natural and urban canopies," in *Flow and Transport Processes with Complex Obstructions*, edited by Gayev, Y. A. and Hunt, J. C. (Springer, 2007), Vol. **236**.
- Motlagh, S. Y. and Taghizadeh S., "Pod analysis of low Reynolds turbulent porous channel flow," *Int. J. Heat Fluid Flow* **61**, 665–676 (2016).
- Nakayama, A. and Kuwahara, F., "A macroscopic turbulence model for flow in a porous medium," *J. Fluids Eng.* **121**, 427–433 (1999).
- Nakayama, A. and Kuwahara, F., "A general macroscopic turbulence model for flows in packed beds, channels, pipes, and rod bundles," *J. Fluids Eng.* **130**, 101205 (2008).
- Nield, D. A., "The limitations of the Brinkman-Forchheimer equation in modeling flow in a saturated porous medium and at an interface," *Int. J. Heat Fluid Flow* **12**, 269–272 (1991).
- Nield, D. A., "Alternative models of turbulence in a porous medium, and related matters," *J. Fluids Eng.* **123**, 928–931 (2001).
- Nield, D. A. and Bejan, A., *Convection in Porous Media*, 5th ed. (Springer, Cham, Switzerland, 2017).
- Nield, D. A. and Simmons C. T., "A brief introduction to convection in porous media," *Transp. Porous Media* **130**(1), 237–250 (2019).
- Ochoa-Tapia, J. A. and Whitaker S., "Momentum transfer at the boundary between a porous medium and a homogeneous fluid—I. Theoretical development," *Int. J. Heat Mass Transfer* **38**, 2635–2646 (1995).
- Odenthal, C., Steinmann, W. D., Eck, M., and Laing, D., "The CellFlux storage concept for cost reduction in parabolic trough solar thermal power plants," *Energy Procedia* **46**, 142–151 (2014).
- Patil, S. B. and Chore H. S., "Contaminant transport through porous media: An overview of experimental and numerical studies," *Adv. Environ. Res.* **3**(1), 45 (2014).
- Pedras, M. H. J. and de Lemos M. J. S., "On the definition of turbulent kinetic energy for flow in porous media," *Int. Commun. Heat Mass Transfer* **27**, 211–220 (2000a).
- Pedras, M. H. J. and de Lemos M. J. S., "Macroscopic turbulence modeling for incompressible flow through undeformable porous media," *Int. J. Heat Mass Transfer* **44**, 1081–1093 (2001a).
- Pedras, M. H. J. and de Lemos M. J. S., "Simulation of turbulent flow in porous media using a spatially periodic array and low Re two-equation closure," *Numer. Heat Transfer, Part A* **39**, 35–59 (2001b).
- Pedras, M. H. J. and de Lemos M. J. S., "On the mathematical description and simulation of turbulent flow in a porous medium formed by an array of elliptic rods," *J. Fluids Eng.* **123**, 941–947 (2001c).
- Pedras, M. H. J. and de Lemos M. J. S., "Computation of turbulent flow in porous media using a low Reynolds number $k-\epsilon$ model and an infinite array of transversely displaced elliptic rods," *Numer. Heat Transfer, Part A* **43**, 585–602 (2003).
- Pirozzoli, S., De Paoli M., Zonta F., and Soldati A., "Towards the ultimate regime in Rayleigh-Darcy convection," *J. Fluid Mech.* **911**, R4 (2021).
- Prescott, P. J. and Incropera F. P., "The effect of turbulence on solidification of a binary metal alloy with electromagnetic stirring," *J. Heat Transfer* **117**, 716–724 (1995).
- Quintard, M. and Whitaker S., "Transport in ordered and disordered porous media: Volume-averaged equations, closure problems, and comparison with experiment," *Chem. Eng. Sci.* **48**(14), 2537–2564 (1993).
- Rao, F. X. and Jin Y., "Possibility for survival of macroscopic turbulence in porous media with high porosity," *J. Fluid Mech.* **937**, A17 (2022).
- Rao, F. X., Kuznetsov A. V., and Jin Y., "Numerical modeling of momentum dispersion in porous media based on the pore scale prevalence hypothesis," *Transp. Porous Media* **133**(2), 271–292 (2020).
- Rosti, M. E., Brandt, L., and Pinelli, A., "Turbulent channel flow over an anisotropic porous wall—drag increase and reduction," *J. Fluid Mech.* **842**, 381–394 (2018).
- Rosti, M. E., Cortelezzi, L., and Quadrio, M., "Direct numerical simulation of turbulent channel flow over porous walls," *J. Fluid Mech.* **784**, 396–442 (2015).
- Rocamora, F. D. and de Lemos, M. J. S., "Analysis of convective heat transfer for turbulent flow in saturated porous media," *Int. Commun. Heat Mass Transfer* **27**, 825–834 (2000).
- Rubinstein, J., "Effective equations for random porous media with a large number of scales," *J. Fluid Mech.* **170**, 379–383 (1986).
- Saez, A. E., Perfetti J. C., and Rusinek I., "Prediction of effective diffusivities in porous media using spatially periodic models," *Transp. Porous Media* **6**, 143–157 (1991).
- Shams, A., Roelofs F., Komen E., and Baglietto E., "Large eddy simulation of a randomly stacked nuclear pebble bed," *Comput. Fluids* **96**, 302–321 (2014).
- Silva, R. A. and de Lemos M. J. S., "Turbulent flow in a channel occupied by a porous layer considering the stress jump at the interface," *Int. J. Heat Mass Transfer* **46**, 5113–5121 (2003).
- Soulaire, C., Quintard M., Baudouy B., and Van Weelder R., "Numerical investigation of thermal counterflow of He II past cylinders," *Phys. Rev. Lett.* **118**, 074506 (2017).
- Srikanth, V., Huang C.-W., Su T. S., and Kuznetsov A. V., "Symmetry breaking of turbulent flow in porous media composed of periodically arranged solid obstacles," *J. Fluid Mech.* **929**, A2 (2021).
- Sun, Y., Kharaghani A., and Tsotsas E., "Micro-model experiments and pore network simulations of liquid imbibition in porous media," *Chem. Eng. Sci.* **150**, 41–53 (2016).
- Uth, M.-F., Jin Y., Kuznetsov A. V., and Herwig H., "A direct numerical simulation study on the possibility of macroscopic turbulence in porous media: Effects of different solid matrix geometries, solid boundaries, and two porosity scales," *Phys. Fluids* **28**, 065101 (2016).
- Vafai, K., *Handbook of Porous Media*, 2nd ed. (Taylor and Francis Group, Boca Raton, 2005).
- Vafai, K. and Tien C. L., "Boundary and inertia effects on flow and heat transfer in porous media," *Int. J. Heat Mass Transfer* **24**, 195–203 (1981).
- Vafai, K. and Tien C. L., "Boundary and inertia effects on convective mass transfer in porous media," *Int. J. Heat Mass Transfer* **25**, 1183–1190 (1982).
- Valdes-Parada, F. J., Alberto Ochoa-Tapia J., and Alvarez-Ramirez J., "On the effective viscosity for the Darcy-Brinkman equation," *Physica A* **385**, 69–79 (2007).
- Wang, W., Chu X., Lozano-Duran A., Helmig R., and Weigand B., "Information transfer between turbulent boundary layers and porous media," *J. Fluid Mech.* **920**, A21 (2021).
- Wang, W., Lozano-Duran A., Helmig R., and Chu X., "Spatial and spectral characteristics of information flux between turbulent boundary layers and porous media," *J. Fluid Mech.* **949**, A16 (2022).
- Wen, B., Corson, L. T., and Chini, G. P., "Structure and stability of steady porous medium convection at large Rayleigh number," *J. Fluid Mech.* **772**, 197–224 (2015).
- Whitaker, S., "The Forchheimer equation: A theoretical development," *Transp. Porous Media* **25**, 27–61 (1996).
- Whitaker, S., *The Method of Volume Averaging* (Kluwer, 1999).
- Wood, B. D., He X. L., and Apte S. V., "Modeling turbulent flows in porous media," *Annu. Rev. Fluid Mech.* **52**, 171–203 (2020).

Wood, B. D. and Valdés-Parada F. J., "Volume averaging: Local and nonlocal closures using a Green's function approach," *Adv. Water Resour.* **51**, 139–167 (2013).

Zhu, J. and Kuznetsov A. V., "Forced convection in a composite parallel plate channel: Modeling the effect of interface roughness and turbulence utilizing a k - ϵ model," *Int. Commun. Heat Mass Transfer* **32**, 10–18 (2005).